THE JOURNAL OF BIOLOGICAL CHEMISTRY
Vol. 278, No. 45, Issue of November 7, pp. 44904–44912, 2003

Printed in U.S.A.

Exploration of the P6/P7 Region of the Peptide-binding Site of the Human Class II Major Histocompatability Complex Protein HLA-DR1*

Received for publication, July 16, 2003, and in revised form, August 27, 2003
Published, JBC Papers in Press, September 1, 2003, DOI 10.1074/jbc.M307652200

Zarixia Zavala-Ruiz‡, Eric J. Sundberg§, Jennifer D. Stone‡, Daniel B. DeOliveira‡, Iat C. Chan‡, Jennifer Svendsen‡, Roy A. Mariuzza§, and Lawrence J. Stern¶‖

From the ‡Massachusetts Institute of Technology, Department of Chemistry, Cambridge, Massachusetts 02139, ¶University of Massachusetts School of Medicine, Pathology Department, Worcester, Massachusetts 01655, and §Center for Advanced Research in Biotechnology, University of Maryland Biotechnology Institute, Rockville, Maryland 20850

Crystal structures of the class II major histocompatibilty complex (MHC) protein, HLA-DR1, generally show a tight fit between MHC and bound peptide except in the P6/P7 region of the peptide-binding site. In this region, there is a shallow water-filled pocket underneath the peptide and between the pockets that accommodate the P6 and P7 side chains. We investigated the properties of this pocket with the idea of engineering substitutions into the corresponding region of peptide antigens to increase their binding affinity for HLA-DR1. We investigated D-amino acids and *N*-alkyl modifications at both the P6 and P7 positions of the peptide and found that binding of peptides to HLA-DR1 could be increased by incorporating an *N*-methyl substitution at position 7 of the peptide. The crystal structure of HLA-DR1 bound to a peptide containing a P7 *N*-methyl alanine was determined. The *N*-methyl group orients in the P6/P7 pocket, displacing one of the waters usually bound in this pocket. The structure shows that the substitution does not alter the conformation of the bound peptide, which adopts the usual polyproline type II helix. An antigenic peptide carrying the *N*-methyl modification is taken up by antigen-presenting cells and loaded onto endogenous class II MHC molecules for presentation, and the resultant MHC-peptide complexes activate antigen-specific T-cells. These results suggest a possible strategy for increasing the affinity of weakly immunogenic peptides that might be applicable to the development of vaccines and diagnostic reagents.

Class II major histocompatibilty complex (MHC)[1] proteins are heterodimeric cell surface proteins that serve as restricting elements for the cell-mediated immune system. Class II MHC proteins bind peptides produced by endosomal proteolysis and present them at the cell surface for recognition by CD4+ T-cell receptors (1, 2). Peptides isolated from class II MHC proteins found in antigen-presenting cells usually contain 15–20 residues (3, 4). The central region of these peptides interact directly with class II MHC proteins, with specific recognition of an ~9-residue stretch (5). Within this binding frame, strong side chain preferences are found in certain positions with weaker preferences at others. Approximately one-third of total peptide surface area in the central region of the peptide is accessible to solvent for recognition by the T-cell receptor.

The binding of peptides to human and mouse class II MHC has been investigated by x-ray crystallography (5–15). The structures reveal several conserved side chain binding pockets within the overall peptide-binding groove (Fig. 1*A*). Generally, these pockets accommodate the side chains of peptide residues at the P1, P4, P6, and P9 positions with smaller pockets or shelves in the binding site accommodating the P3 and P7 residues (the pockets are numbered along the peptide relative to a large usually hydrophobic pocket near the peptide-binding site). The pockets correspond to positions where strong side chain-binding preferences are observed in studies of MHC-peptide interaction (16). Allelic differences in the residues lining the pockets determine the peptide binding specificity (or motif) of the various class II MHC alleles. For example, in HLA-DR1 (DRB1*0101), a common human class II MHC protein, the P1 pocket shows a strong preference for large hydrophobic side chains (Trp, Tyr, Phe, Leu, and Ile), the P6 pocket has a strong preference for small residues (Gly, Ala, Ser, and Pro), and the P4 and P9 pockets have weaker preferences for residues with some aliphatic character (5, 16).

Structures of HLA-DR peptide complexes generally show a tight fit between MHC and peptide. A prominent exception to this is a relatively large region underneath the peptide between the P6 and P7 pockets (Fig. 1). The conformation of peptides bound to class II MHC proteins is tightly restricted to a polyproline type II-like conformation, probably as a result of 12–15 conserved hydrogen bonds between the MHC and peptide main chain (17), and a peptide side chain from a conventionally bound peptide is not likely to bind in this region. Crystal structures of HLA-DR1-peptide complexes reveal that several water molecules were tightly bound underneath the peptide between the P6 and P7 pockets. Four water sites in this region were observed to be variously occupied in lower resolution structures (2.5–2.8 Å) (5, 14, 18). At a higher resolution (1.93 Å), all four waters were observed (19)

As part of an effort to explore ways to increase the binding affinity of antigenic peptides, we attempted to modify known antigenic peptides to take advantage of the P6/P7 void by

* This work was supported by National Institutes of Health R01-AI38996 (to L. J. S.), National Institutes of Health R01-AI369000 (to R. A. M.), and National Institutes of Health F31-GM64859 (to Z. Z. R.). The costs of publication of this article were defrayed in part by the payment of page charges. This article must therefore be hereby marked "*advertisement*" in accordance with 18 U.S.C. Section 1734 solely to indicate this fact.

The atomic coordinates and structure factors (code 1PYW) have been deposited in the Protein Data Bank, Research Collaboratory for Structural Bioinformatics, Rutgers University, New Brunswick, NJ (http://www.rcsb.org/).

‖ To whom correspondence should be addressed: Rm. S2–127, 55 Lake Ave. N., University of Massachusetts School of Medicine, Worcester, MA 01655. Fax: 508-856-0019; E-mail: lawrence.stern@umassmed.edu.

[1] The abbreviations used are: MHC, major histocompatibilty complex; Fmoc, *N*-(9-fluorenyl)methoxycarbonyl; IL, interleukin.

displacing bound water molecules. We wanted to introduce relatively small alterations in the peptide, because the expected application of such modified peptides generally would require cross-reactivity with the native sequence and because T-cell antigen receptors are very sensitive to structural changes in a MHC-bound peptide. Single amino acid substitutions at a T-cell contact residue can abrogate T-cell recognition (20) or convert agonist peptides into antagonists (21). Modifications of the peptide backbone of class II MHC-binding antigens also have been reported in an effort to increase bioavailability or serum half-life and include alkylation, peptide-bond reduction, and incorporation of peptoid, azapeptide, dipeptide mimetic substitutions, and D-amino acids (8, 22–26). In general, peptides carrying one or more of these modifications are less effective T-cell activators as compared with a peptide that does not include the modification (23, 26, 27).

Using the crystal structures as a guide to design P6/P7-binding antigen analogues, we were able to develop a peptide modification strategy that increases MHC-peptide binding affinity by displacement of waters in the P6/P7 region. Crystal structure analysis of MHC-peptide complexes carrying the modification (P7 amide *N*-methylation) confirms that waters were displaced without significant conformational alteration, and T-cell activation studies show that the modification does not affect interaction with the T-cell receptor.

EXPERIMENTAL PROCEDURES

Protein Expression and Purification—For peptide-binding experiments, the extracellular portion of HLA-DR1 was produced from a recombinant baculovirus-infected SF9 insect cells as soluble empty $\alpha\beta$ heterodimers as described previously (28). For x-ray crystallography experiments, extracellular portion of HLA-DR1 was produced by expression of isolated subunits in *Escherichia coli* inclusion bodies followed by refolding *in vitro* in the presence of peptide as described previously (29). Refolded HLA-DR1 protein was purified by immunoaffinity chromatography using the conformation-specific monoclonal antibody LB3.1 and gel filtration in phosphate-buffered saline, pH 6.8. The protein concentration was measured by UV absorbance at 280 nm using ϵ_{280} of 54375 M^{-1} cm^{-1} for empty DR1. SEC3–3B2 was expressed as a soluble protein in *E. coli* and isolated from the periplasmic fraction as described previously (30). SEC3–3B2 is a variant of the SEC3 protein that binds with a higher affinity to the MHC class II molecule, HLA-DR1 (30).

Peptide Synthesis—Peptides were synthesized using solid-phase Fmoc chemistry on an Advanced ChemTech 357 synthesizer. All of the peptides were synthesized containing an acetylated N terminus and an amidated C terminus to prevent possible effects of charged termini in the binding site with the exception of *N*-biotinylated peptides, which were produced by coupling aminocaproyl-(LC)-biotin succinimide ester (Pierce) to the N terminus of the resin-bound, side chain-protected peptide. The peptides were deprotected and cleaved from the resin by a 3-h treatment at room temperature with a mixture of trifluoroacetic acid/H_2O/dithiothreitol/triisopropylsilane (88:5:5:5:2.5). The solution of peptides was filtered into cold diethyl ether, and the precipitated peptides were filtered, washed with ether, and dried in vacuum. The crude peptides were purified by high performance liquid chromatography (Vydac-C18). The purity and homogeneity of each peptide was checked by high performance liquid chromatography (Vydac-C18) and matrix-assisted laser desorption ionization time-of-flight mass spectrometry. Peptide concentration was measured by absorbance using high pressure liquid chromatography-UV detection at 280 and 254 nm for peptides containing Tyr and Phe residues, respectively. *N*-Methyl amino acids were purchased as protected amino acid precursors and coupled in the usual manner. For the other *N*-substitutions, the *N*-substituted residue was generated piecemeal on the resin with conventional Fmoc/1,3-diisopropylcarbodiimide/*N*-hydroxy-benzotriazole chemistry used to make the fore and aft parts of the peptide following a "submonomer" strategy used previously for generating *N*-substituted glycines (31, 32). At the *N*-alkyl residue, the glycine backbone was first introduced using bromoacetic acid coupled twice with 1,3-diisopropylcarbodiimide and then the *N*-substitution was added as an alkylamine (or Boc-aminoalkylamine) by nucleophilic displacement for 2 h at 37 °C. The next amino acid was coupled using a PyBrop/diisopropylethylamine activation strategy with triple coupling for 120 min. The remainder of the sequence was prepared normally. We attempted similarly to prepare *N*-substituted alanines using bromopropionic acid, but we were unable to efficiently couple the subsequent residue. The *N*-alkyl peptides were deprotected and purified in the usual manner.

IC_{50} Determination—A competition assay was used to determine binding affinities of peptides. Peptide-free DR1 produced in insect cells (10 nM) was mixed with biotinylated Ha-(306–318) probe (10 nM) and varying concentrations of unlabeled competitor peptide. The mixtures were incubated for 3 days at 37 °C in phosphate-buffered saline buffer containing 0.02% NaN_3 followed by detection of bound biotinylated peptide using an immunoassay that employed an anti-DR1 capture antibody LB3.1 and streptavidin-Eu detection (33). IC_{50} values were obtained by fitting a binding curve to the plots of fluorescence *versus* concentration of competitor peptide. The K_D of the biotinylated Ha probe peptide is ~10 nM (34, 35).

HA1.7 T-cell Hybridoma Activation Assay (IL-2 Production)—We used a mouse T-cell hybridoma transfected with a chimeric T-cell receptor carrying human variable α and β domains from the well characterized HLA-DR1-restricted Ha-peptide-specific human T-cell clone HA1.7 (36) and murine constant domains. The T-cell hybridoma was developed as an indicator cell for productive MHC-T-cell receptor interactions and produces IL-2 upon receptor engagement (37).

In some experiments, HA1.7 hybridoma cells were incubated with purified MHC-peptide complexes immobilized on the polystyrene assay plate for 24 h at 37 °C. Culture supernatant was tested for IL-2 production using a murine IL-2 detection sandwich enzyme-linked immunosorbent assay kit (PeproTech). In other experiments, antigen-presenting cells pre-pulsed with peptide were used as stimulators. For antigen-presenting cells, we used LG2, a DR1+ homozygous Epstein-Barr virus-transformed B cell line. Live or fixed (1% paraformaldehyde) LG2 cells (5.0×10^4 cells/well) were pulsed with varying concentrations of peptide (10^{-9} to 10^{-5} M) in serum-free medium in a round-bottom 96-well plate for 2 h at 37 °C. The peptide was washed away, and the LG2 cells were resuspended in suspension-minimal essential medium (used for routine passage of HA1.7 hybridoma cells). HA1.7 hybridoma cells were added to wells (10^5 cells/well) with peptide-pulsed LG2 cells and incubated for 24 h at 37 °C. Supernatant was tested for IL-2 production as described above.

Crystallization—HLA-DR1-peptide bound complex was prepared by incubating purified empty HLA-DR1 (1–5 μM) with at least 5-fold molar excess peptide for 3 days at 37 °C in phosphate-buffered saline with 0.02% sodium azide. The complex was purified by gel filtration to remove aggregates and free peptide. Purified HLA-DR1/peptide complex was mixed in equimolar ratio with purified SEC3–3B2. Crystals of HLA-DR1/Ac-FVKQNAAAL-NH_2/SEC3–3B2 were grown by the vapor diffusion method in hanging drops. The crystals grew at 4 °C under the following conditions: 2–6% polyethylene glycol 4000, 10% ethylene glycol, 100 mM sodium acetate, pH 5.2–5.6, and 1μl of precipitant solution mixed with 1μl of 8 mg/ml protein complex. For x-ray diffraction experiments, the crystals were soaked for ~1 min in a cryoprotectant solution consisting of 25% ethylene glycol in the mother liquor and then flash-cooled in liquid nitrogen.

Data Collection and Processing—A high resolution data set (2.1 Å) was collected for a single crystal (200 μm × 150 μm × 150 μm) on a Mar345 image plate detector using CuKα radiation from a rotating anode source. Collected data were processed and scaled using Denzo, Scalepack, and the CCP4 package (38, 39). An overall isotropic B factor was estimated to be 21.6 Å from a Wilson plot.

Structure Determination—The structure of the complex was determined by molecular replacement. HLA-DR1/$TPI_{23–37}$/SEC3–3B2 (Protein Data Bank code 1KLU) was used as the search model to find a molecular replacement solution (19). The peptide and waters were removed from the model. Refinement was carried out using CNS (40). After initial rigid-body refinement, three rounds of refinement included minimization, B-factor, and minimization. After each round, the protein was inspected using program O and XtalView (41, 42). Waters were added to the refined molecule using CNS. N-terminal acetyl group, C-terminal amide group, and the *N*-methyl group at the P7 position were included in the peptide model using data generated by the Dundee PRODRG server (43). The final model was verified for distortions on the secondary structures features using Procheck (44).

RESULTS

D-Amino Acids in P6 and P7 Positions—To investigate the binding properties of the HLA-DR1 P6/P7 pocket, we initially substituted D-amino acids into the P6 and P7 positions of a known HLA-DR1-binding peptide and measured the effects of

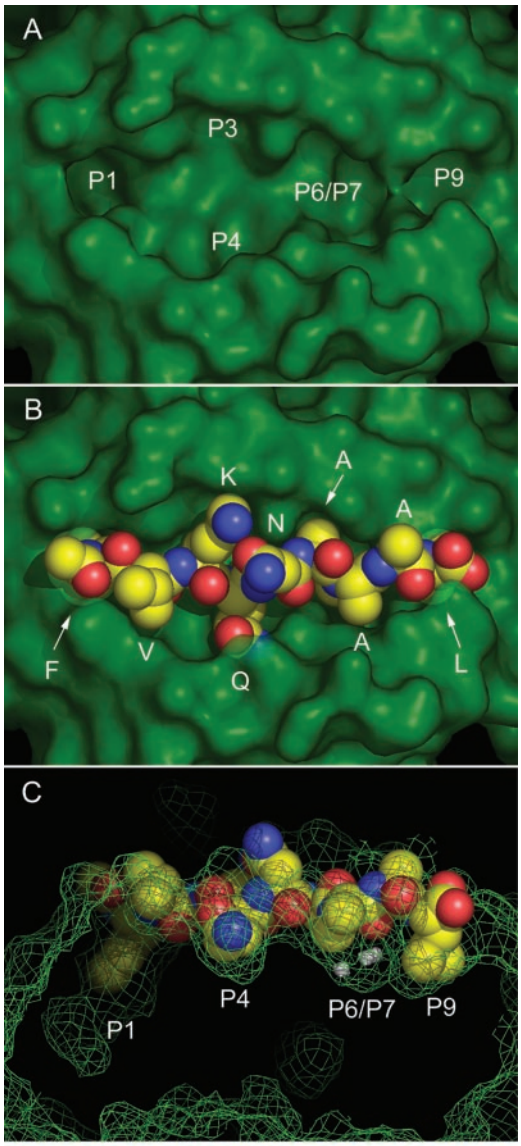

FIG. 1. **Pockets in the peptide binding site of HLA-DR1.** *A*, surface of the HLA-DR1-peptide binding site with side chain binding pockets within the overall peptide-binding site labeled according to the peptide side chain accommodated. The region under investigation in this study between the P6 and P7 pockets is labeled *P6/P7*. *B*, same view as *A* with bound FVKQNAAAL (*A* = *N*-methyl alanine) peptide as a Corey-Pauling-Koltun model. Carbon atoms are *yellow*; nitrogen atoms are *blue*; and *oxygen* atoms *red*. *C*, *side view* of the peptide-binding site, showing water molecules (*white*) bound underneath the peptide in the P6/P7 region. The surface is shown as a *green mesh*, and the view is rotated 90° around the horizontal axis relative to that of *B*. Figures were generated using PyMol (68).

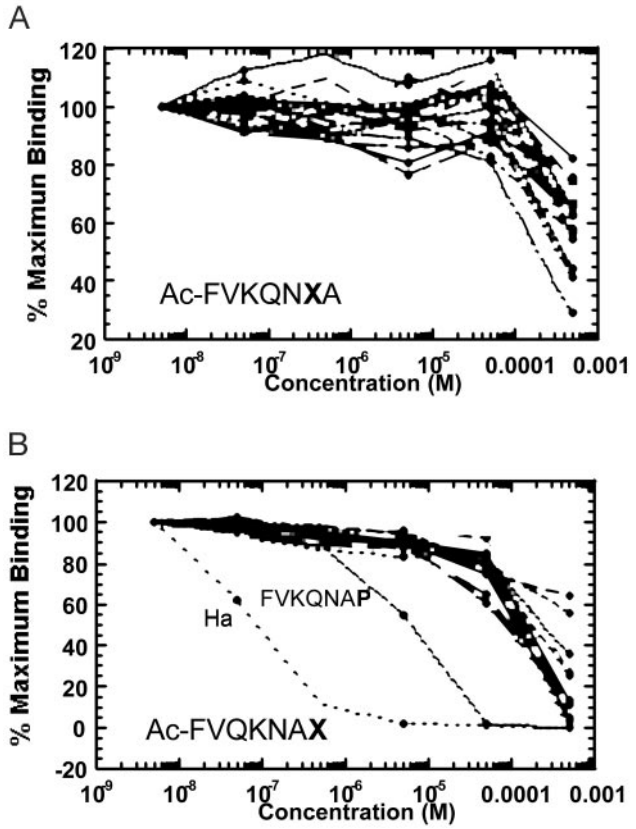

FIG. 2. **Effect of D-amino acids at position 6 or 7 of the Ha peptide analogue.** *A*, competitive-binding analysis of peptides with D-amino acids at the P6 position. A fixed concentration of peptide-free HLA-DR1 and biotinylated Ha peptide was incubated with increasing concentrations of Ac-FVKQNxA peptides having various D-amino acid residues at the P6 position (see "Experimental Procedures"). After binding for 3 days at 37 °C, the amount of bound bio-Ha peptide/HLA-DR1 complexes was measured using a streptavidin europium assay. *B*, competitive-binding analysis of peptides with D-amino acids at P7. Of 38 D-amino acid residues tested at P6 and P7, only D-Pro (P7) substantially increased the binding affinity of the base peptide.

the substitutions on peptide binding affinity using a competition assay. Naturally occurring L-amino acid containing sequences orient the P6 and P7 residues into the side chain-binding pockets that flank this region (P6 and P7, Fig. 1, *A* and *B*), leaving the P6/P7 pocket open to be filled by several water molecules (Fig. 1*C*). We reasoned that a peptide containing a D-amino acid at either position might be able to position a side chain into the pocket. The template peptide NH_2-FVKQNAA-$CONH_2$ was designed as a scaffold for the substitutions. The peptide is based on the central region of the viral peptide PKYVKQNTLKLAT (Ha306–318) (5, 18, 34, 36) derived from the influenza virus hemagglutinin. The original peptide length was reduced from 13 residues, 11 of which are bound by HLA-DR1, to 7 residues, to emphasize the interactions of interest in the P6/P7 region while maintaining the original binding frame that places an aromatic residue in the P1 position. The five N-terminal residues FVKQN of the scaffold peptide correspond to the native Ha sequence with the exception that an original tyrosine at position 1 was changed to phenylalanine to reduce the relative importance of the P1 pocket while maintaining the original binding frame. The Ala-Ala sequence at positions 6–7 was originally Thr-Leu. These were substituted to alanine to provide a rational basis for comparison of the D-amino acids. Finally, the N and C termini were acetylated and amidated, respectively, to prevent ionization of the termini that might disrupt the conserved hydrogen-bonding arrangement that constrains the peptide in the binding site. Effects of introduction of peptide D-amino acids to the MHC-peptide binding affinity have been investigated previously by other groups (24, 26).

38 D-amino acid substitutions were introduced at the P6 and P7 positions of the FVKQNAA test peptide (Fig. 2). Substitutions with D-amino acids were made at position 6 holding position 7 constant with L-alanine (Fig. 2*A*) and conversely at position 7 holding position 6 constant with L-alanine (Fig. 2*B*). 19 D-amino acids were tested at each position (D-analogs of all naturally occurring amino acids with the exception of D-Ile and D-Cys were included in the library along with D-ornithine). Of the 38 D-amino acid substitutions tested, only D-Pro at position 7 was found to increase the binding affinity of the base peptide.

Peptide	IC_{50}(nM)	Peptide	IC_{50}(nM)
FVKQN	400,000	YTALA	8000
FVKQNAA	15,000	YTALAAA	20
FVKQNAAAA	108	YTALAAAAA	22
FVKQNAAAL	90	YTALAAAAL	<1
FVKQNAP	1430	YTALAAP	46
FVKQNAPAA	31	YTALAAPAA	2
FVKQNAPAL	34	YTALAAPAL	≤1
FVKQNA**P**	8000	YTALAA**P**	12
FVKQNA**P**AA	20,000	YTALAA**P**AA	700
FVKQNA**P**AL	20,000	YTALAA**P**AL	129
123456789		123456789	

P = D-proline

FIG. 3. **Effect of peptide extension beyond D-Pro at position 7.** IC_{50} values from a competitive binding assay (as Fig. 2) for peptides that include extensions beyond the P7 position.

Peptide	IC_{50}(nM)	Peptide	IC_{50}(nM)
FVKQNAA	15,000	FVKQNAG	278,000
FVKQNA<u>A</u>	2,000	FVKQNA<u>G</u>	50,000
FVKQNA<u>A</u>AA	70	FVKQNA<u>G</u>AA	2000
FVKQNA<u>A</u>AL	20	FVKQNA<u>G</u>AL	500
123456789		123456789	

<u>A</u> = N-methyl alanine
<u>G</u> = N-methyl glycine

FIG. 4. **Extension beyond an *N*-methyl residue at position 7.** IC_{50} values from a competitive binding assay for peptides carrying *N*-methyl glycine and *N*-methyl alanine at P7.

The peptide Ac-FVKQNA**P**-NH_2 (where **P** = D-proline) exhibited IC_{50} of 8 μM (K_d ~4 μM, see "Experimental Procedures"), binding 20–100-fold more tightly than the other sequences.

We confirmed this result in the context of a different base peptide, YTALAAA (Fig. 3). This peptide binds ~10^3-fold more tightly than FVKQNAA, because it carries the residues most favorable for HLA-DR1 binding at the key P1, P4, and P6 positions (16) as well as a threonine at position 2, which can make a favorable interaction with the MHC backbone (11). P3 and P5, both alanines in this peptide, are primarily T-cell contacts and do not contribute significantly to the MHC-peptide binding affinity (18). YTALAA**P** binds tightly to HLA-DR1 relative to the already tightly binding YTALAAA, indicating a positive contribution to the binding of D-Pro at position 7 in this peptide, similarly to that observed for FVKQNA**P** (Fig. 3). As similar effects were observed for D-Pro at position 7 in the context of two completely different sequences, we concluded that the incorporation of an alkyl group at the nitrogen group of the P7 residue can increase peptide binding to HLA-DR1.

Surprisingly, incorporation of D-Pro at position 7 prevented productive C-terminal extension of the peptide. Peptides ending with either D-Pro or L-Pro at position 7 bind similarly, but longer peptides having a D-Pro at P7 bind 100–500-fold worse than the corresponding L-Pro-containing peptides. This appears to be the result of the inability of D-Pro-containing peptides to make use of productive interactions in the P8-P10 region, probably because of alterations to the peptide backbone conformation induced by binding a side chain in the D conformation into a pocket adapted to L-amino acid residues. In general, C-terminal extensions of conventional L-amino acid-containing peptides lead to substantial increases in peptide binding affinity. This is attributed to the contribution of MHC-peptide main chain hydrogen bonds in the P8-P10 region together with occupancy of the P9 pocket (specific for residues with aliphatic side chains). However, in both the FVKQA and YTALA series, C-terminal extension beyond the D-Pro at position 7 by the usually favorable Ala-Ala and Ala-Leu sequences led to a substantial decrease in binding affinity. The addition of Ala-Ala or Ala-Leu beyond a C-terminal L-Pro increased the binding affinity by 20–40-fold for the various peptides, whereas the addition beyond D-Pro in the same sequences decreased the affinity by 2.5 to >50-fold (Fig. 3).

The inability to productively extend D-Pro-containing peptides could be due to the constraints of the Pro ring in the D-form, which might prevent the peptide C-terminal portions from adopting the canonical polyproline type II conformation (approximately three residues per turn with a right-handed twist) that has been observed in all class II MHC crystal structures determined to date. In this scenario, the peptide main chain of L-Pro-containing peptides can adopt the polyproline type II conformation, thus maintaining key hydrogen-bonding contacts and occupation of the P9 pocket. Peptides that contain a D-Pro, however, would direct the C-terminal main chain of peptides out of the binding groove because of the opposite orientation of the constrained ring and thus would lose binding affinity. Since none of the other D-amino acids at position 7 provides any substantial binding affinity, we tentatively ascribed the positive effects on peptide binding at P7 to the *N*-alkyl portion of the D-Pro side chain and the negative effects on productive peptide extension to the constraints introduced by the five-membered proline ring.

N-Methyl Alanine and N-Methyl Glycine at P7—To deter-

mine whether the *N*-alkyl portion is in fact responsible for the increase in binding affinity observed upon D-Pro substitution, we decided to mimic the δ-CH_2 moiety by incorporating amino acids that contain an *N*-methyl substituent at the P7 position. To this end, FVKQNAA peptides containing *N*-methyl alanine or *N*-methyl glycine (sarcosine) at P7 were synthesized and evaluated for HLA-DR1 binding. Peptides containing *N*-methyl alanine or *N*-methyl glycine bound 7.5- and 5.5-fold more tightly than those containing the corresponding natural amino acid residues (Fig. 4). The 9-mer peptide FVKQNA*A* (*A* = *N*-methyl alanine; IC_{50} = 2 μM) had similar affinity as did the FVKQNA**P** sequence (**P** = D-Pro; IC_{50} = 8 μM), supporting the idea that the *N*-alkyl substituent is a key determinant of the affinity increase. Moreover, both *N*-methyl glycine and *N*-methyl alanine peptides could be extended with concomitant increases in binding affinity, suggesting that they bind productively in the normal conformation (Fig. 4).

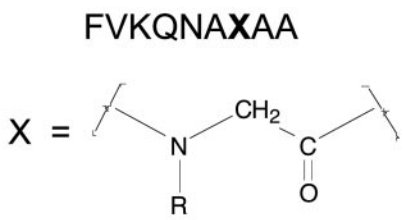

Substitution	IC_{50} (nM)
R=	
$-CH_3$	2,000
$-CH_2CH_3$	3,000
$-CH(CH_3)_2$	3,100
$-(CH2)_2NH_3$	19,000
$-(CH_2)_3NH_3$	31,000
$-(CH_2)_4NH_3$	9,600

FIG. 5. ***N*-Alkyl substitution of the P7 residue.** IC_{50} values from a competitive binding assay when different alkyl groups are used as *N*-substitutions at the P7 position.

N-Substituted Glycine at P7—To determine whether *N*-substituted groups larger than methyl could be accommodated in the P6/P7 pocket, we synthesized peptides containing additional substituents on the amide nitrogen of the P7 residue and evaluated their binding to HLA-DR1. The substituents included linear and branched aliphatic chains designed to identify whether the P6/P7 pocket would be able to accommodate groups larger than methyl and linear aliphatic amines designed to be complementary to the generally acidic electrostratic character of the P6/P7 region. The *N*-substituted residue was generated *in situ* on the resin using a submonomer strategy previously described for generation of *N*-substituted glycines (31, 32) with conventional Fmoc chemistry used to make the fore and aft parts of the peptide. We attempted but were unable to extend this methodology to generation of *N*-substituted alanines (see "Experimental Procedures"). None of the *N*-alkyl substitutions (ethyl, isopropyl, aminoethyl, aminopropyl, and aminobutyl) increased the binding affinity over that observed for the *N*-methyl substitution (Fig. 5), suggesting that larger is not necessarily better in the P6/P7 pocket.

Crystal Structure of N-Methyl Alanine at P7—To evaluate whether the *N*-methyl substitution introduced any unexpected alteration of the peptide conformation and to determine the nature of the constraint on the size of the *N*-alkyl moeity, the crystal structure of the peptide Ac-FVKQNAAAL-NH_2 (*A* =

TABLE I
Data collection and refinement statistics

Crystal parameters			
Space group	R3		
Cell dimensions			
a (Å)	172.50		
c (Å)	121.65		
Data collection	Overall	Highest resolution shell	
Resolution limits (Å)	20.0–2.10	2.17–2.10	
Unique reflections	79,802	7,968	
Total reflections	366,342	32,165	
Completeness (%)	100.0	99.9	
Mean $I/\sigma[\rho]$ (I)	11.5	3.5	
R_{sym}(%)[a]	7.5	39.4	
Refinement			
R_{free}[b]	23.0	31.2	
R_{crys}[b]	20.5	28.4	
Model[c]	Number of residues (atoms)	Average B-factor	Real space R_{factor}[d]
		$Å^2$	
HLA-DR1	368 (3026)	32.5	0.063
Peptide	7 (67)	22.9	0.030
SEC3–3B2	229 (1883)	31.0	0.063
Waters	414	34.9	0.095
Ramachandran plot statistics			
Core + allowed (%)	99.6		
Generous (%)	0.4		

[a] $R_{sym} = \Sigma I - \langle I\rangle/\sigma\langle I\rangle$, where I is the observed intensity and $\langle I\rangle$ is the average intensity of multiple symmetry-related reflections, and the summation taken over all of the multiple-recorded reflections (average redundancy 4.6).

[b] Reciprocal space $R_{factor} = \Sigma F_{obs} - F_{calc}/\Sigma F_{obs}$ with the summation taken over 10% of reflections omitted from the refinement and used as a test set (R_{free}) or else the remaining 90% of reflections used in the refinement (R_{cryst}).

[c] The atomic coordinates for the crystal structure of this protein are available in the Research Collaboratory for Structural Bioinformatics Protein Data Bank 1PYW.

[d] Real space $R_{factor} = (\Sigma\rho_{obs} - \rho_{calc})/(\Sigma\rho_{obs} + \rho_{calc})$ with the summation taken over the space occupied by the molecule. The function describes the fit between the model and the electron density map.

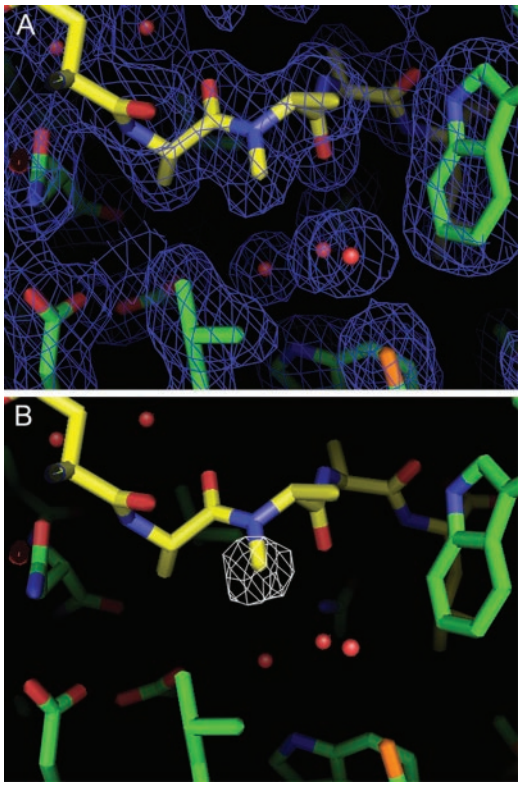

FIG. 6. **Electron density maps for the P6/P7 region of HLA-DR1/FVKQNAAAL/SEC3–3B2.** *A*, composite omit $F_o - F_c$ electron density map contoured at 1σ using data in the resolution range of 20–2.1 Å. HLA-DR1 carbon atoms are *colored* in *green*, FVKQNAAAL peptide carbon atoms are in *yellow*, nitrogen and oxygen are *blue* and *red*, respectively. Waters are represented as *small red spheres*. In a composite omit map, all of the atoms are sequentially omitted from the calculation to reduce model bias (40). *B*, difference $F_o - F_c$ electron density map with the *N*-methyl group of the P7 position of peptide omitted from the map calculation contoured at 3σ. Figures were generated using PyMol (68).

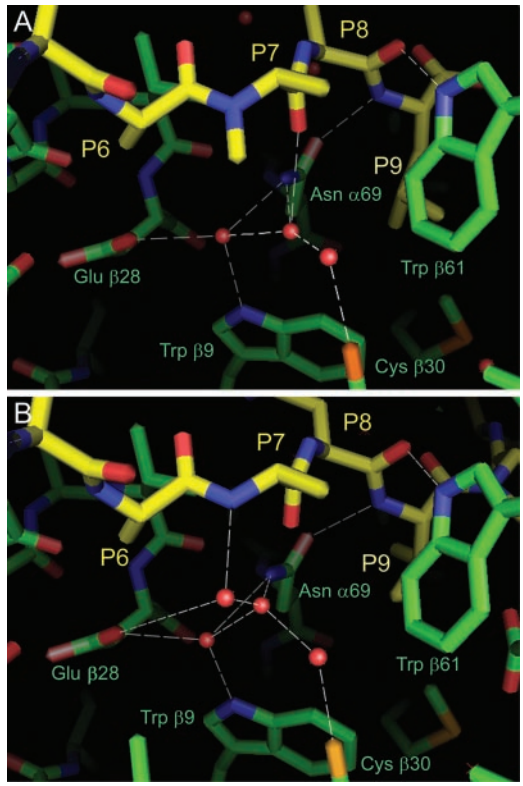

FIG. 7. **Comparison of the hydrogen bond network in the P6/P7 region of peptide-binding site for peptides with and without *N*-methyl group at P7.** *A*, hydrogen bond network for HLA-DR1/FVKQNAAAL/SEC3–3B2 in the P6/P7 region (*colored* as in Fig. 6). *B*, hydrogen bond network for HLA-DR1/$TPI_{23–37}$/SEC3–3B2 ($TPI_{23–37}$ sequence GRLIGTLNAALVPAD) (19) in the P6/P7 region.

N-methyl alanine) bound to HLA-DR1 was determined at 2.1 Å. The complex was crystallized in the presence of the superantigen SEC3–3B2. Superantigens are a class of disease-causing proteins of viral or bacterial origin that hyperactivate the immune system by cross-linking MHC proteins and T-cell receptors (45) and which have been used successfully as an aid to crystallization of HLA-DR-peptide complexes (8, 19). Here we have used the affinity-matured 3B2 variant of staphylococcal enterotoxin SEC3 (30), which interacts with HLA-DR1 outside the binding groove on the flanking helix from the α-subunit (46). MHC-peptide-superantigen crystals, grown under previously determined conditions (19), were used for x-ray data collection at −100 °C. Diffraction data to 2.1 Å were collected using an Mar345 image plate detector and a CuK_α x-ray source (Table I). Initial phases were obtained by molecular replacement using as a search model another HLA-DR1/SEC3–3B2 complex (Protein Data Bank code 1KLU) (19) with peptide coordinates removed followed by a few rounds of manual rebuilding and refinement (see "Experimental Procedures" for details).

Electron density for HLA-DR1 was interpretable and continuous throughout the molecule with the exception of residues 112–113 that were in a loop at the distant region of the β-chain and away from the peptide-binding site. In the case of SEC3–3B2, the electron density was clear and continuous with the exception of residues 97–105 for which no interpretable density was seen. Clear density can be seen for all of the peptides including the *N*-methyl group from the P7 residue (Fig. 6). *N*-Methyl density can be seen in a standard $2F_o - F_c$ composite omit map (Fig. 6*A*) and particularly clearly in a $F_o - F_c$ difference omit map calculated with the *N*-methyl group omitted (Fig. 6*B*). In this case, the *N*-methyl peak is the most prominent feature of the map.

In the structure of a related complex carrying a normal non-methylated peptide, DR1/$TPI_{23–37}$/SEC3–3B2 (19), four waters bind in the P6/P7 area of the peptide-binding groove and participate in a network of hydrogen bonds (Fig. 7*B*). These same waters are observed in other HLA-DR1 structures determined at lower resolution, although not every water is observed in each structure. One of these waters normally makes a hydrogen bond with the nitrogen of the peptide backbone at the P7 position (Fig. 7*B*). This water is displaced by the introduction of the *N*-methyl group at the P7 position of the peptide (Fig. 7*A*). The hydrogen bond network linking the other water molecules in the area adjusts slightly in response to the perturbation. With the exception of this change, no other significant structural alteration appears to result from the *N*-methyl substitution.

T-cell Activation Assay—To assess the effect of *N*-methylation of the P7 residue on recognition by T-cells, the substitution was incorporated into the native antigenic peptide (Ha306–318) derived from influenza hemagglutinin (36). In the context of this peptide, which binds very tightly (34), no significant improvement of binding affinity to HLA-DR1 was observed as a result of the *N*-methyl introduction (Fig. 8*A*). The corresponding MHC-peptide complexes were used to activate a T-cell hybridoma carrying a HLA-DR1-restricted Ha306–318-specific T-cell receptor with the induction of IL-2 secretion used to monitor T-cell activation (8). HLA-DR1 complexes of both the native Ha peptide and Ha7 *N*-CH_3 peptide were able to simi-

A

Peptide	Sequence 1 4 67 9	IC_{50} (nM)
Ha	PKYVKQNTLKLAT	10
Ha 7 N-CH_3	PKYVKQNTL̲KLAT	7

L̲ = N-Methyl leucine

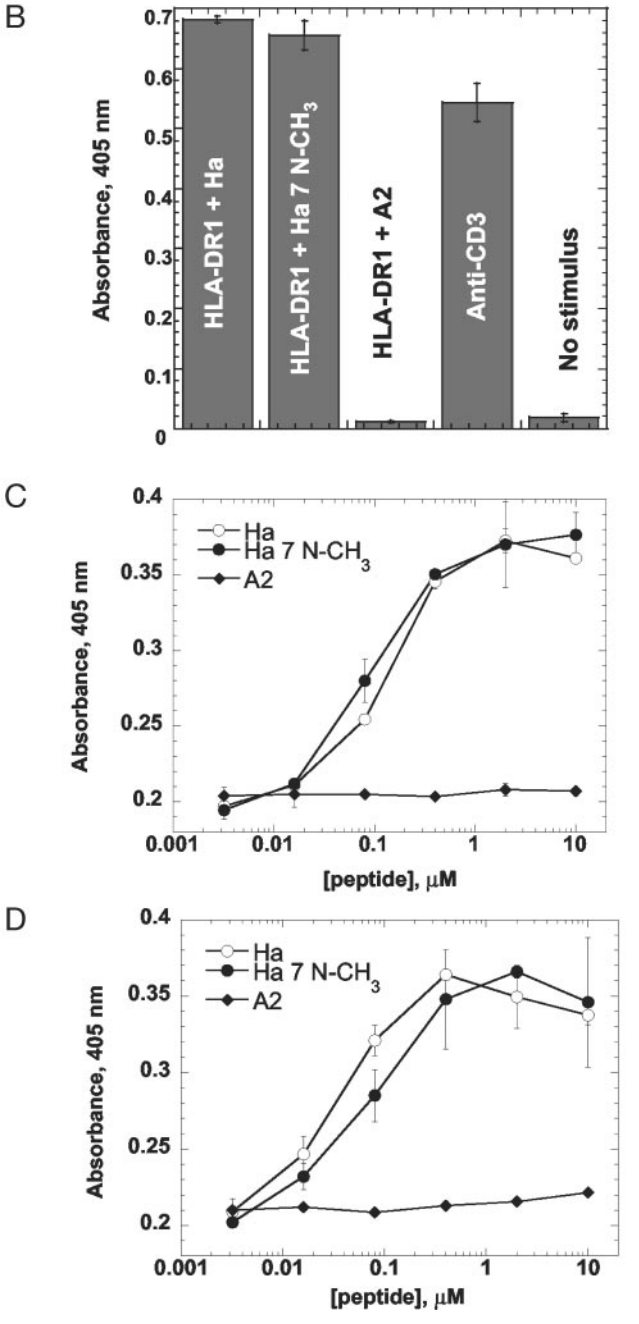

FIG. 8. **Peptide binding data and HA1.7 T-cell hybridoma assays for Ha and Ha7 N-CH_3 peptides.** *A*, peptide sequences and IC_{50} values calculated from a competitive-binding assay for native and *N*-methyl P7 variant of the influenza hemagglutinin Ha peptide. *B*, response of HLA-DR1-restricted Ha-specific T-cell hybridoma to immobilized MHC-peptide complexes. The peptide A2 used as a negative control derives from the class I MHC protein HLA-A2 (4). Immobilized anti-CD3 antibody was used as a positive control for T-cell activation. T-cell activation was measured by an enzyme-linked immunosorbent assay for secreted IL-2. C, response of the T-cell hybridoma to MHC-peptide complexes presented at the surface of antigen-presenting cells. Fixed B cells from an HLA-DR1-expressing line were incubated with Ha peptide (*open circles*), Ha7 N-CH_3 peptide (*filled circles*), or negative control A2 peptide (*diamonds*) in order to load cell-surface MHC molecules. After loading, the B cells were washed and assayed for their ability to induce T-cell activation as in *panel B*. *D*, T-cell activation assay performed as in *panel C* with the exception that peptide was added to live B cells.

larly stimulate the T-cell hybridoma, whereas an irrelevant peptide complex was inactive (Fig. 8*B*). We tested the ability of the *N*-methylated peptide to be presented by cell-surface MHC molecules as normally expressed by antigen-presenting cells. Native and modified peptides were added to antigen-presenting cells (an Epstein-Barr virus-transformed B-cell line) that express endogenous HLA-DR1 to allow cellular binding and presentation. Both native Ha peptide and Ha7 *N*-CH_3 were presented effectively to T-cells by fixed (Fig. 8*C*) or live (Fig. 8*D*) antigen-presenting cells. These experiments indicate that the *N*-methyl introduction does not interfere with the ability of the Ha peptide to be presented by cellular MHC proteins or to activate T-cells.

DISCUSSION

Class II MHC proteins, together with their bound antigenic peptides, are the ligands for antigen receptors on CD4+ T-cells. The interaction is an important part of the process that triggers inflammatory and antibody-mediated immune responses to foreign antigens in the body, and peptide antigens represent a possible target for design of immunotherapeutic agents. Approaches to peptide-based immunotherapeutic agents include attempts to design MHC-binding antigens with improved bioavailability (8), altered T-cell response (47), and stabilized MHC-peptide interaction (48). The last approach is potentially important for the development of MHC-peptide complexes able to induce immunological tolerance in autoreactive T-cells, which frequently recognize weakly binding peptides (49–51).

As a step toward the development of a strategy for stabilizing MHC-peptide interaction without abrogating T-cell receptor recognition, we have investigated the P6/P7 region of the human class II MHC protein HLA-DR1 using as a model antigen the antigenic peptide Ha (308–316) derived from influenza hemagglutinin. This region underneath the peptide and between the MHC pockets that bind the side chains of peptides P6 and P7 is one of the few areas of shape non-complementarity in the overall binding site. In crystal structures of several HLA-DR1 peptide complexes, water molecules are found in this region, making hydrogen-bonding interactions with each other and with MHC side chain and peptide main chain groups. We investigated the ability of D-amino acid side chains at P6 and P7 to bind into the P6/P7 pocket. Only D-Pro at position P7 increased the binding affinity over a P7 glycine residue. Structural constraints on the peptide conformation prevented P7 D-Pro-containing peptides from interacting productively with the MHC beyond the P7 position, but *N*-methylation of the P7 amide provided increased binding due to interactions in the P6/P7 region while at the same time allowing the native peptide polyproline conformation. Crystal structure analysis verified that the *N*-methyl substitution bound in the P6/P7 region by displacing one of the bound water molecules without appreciable alteration of the peptide structure elsewhere. T-cell activation studies confirmed that the native antigenic T-cell receptor interaction was not altered by the modification.

Displacement of bound water molecules is thought to promote ligand binding through favorable entropic effects on the free energy. Improved inhibitors of human immunodeficiency virus protease (52), FK506-binding protein (53), glycogen phosphorylase (54), and cholera toxin (55) have been designed based

on this principle. However, displacement of bound water molecules can have enthalpic consequences as well, including loss of favorable bridging interactions (56, 57) and alteration of protein ionization potentials (58). Moreover, displacement of bound water can result in protein or ligand conformational changes with corresponding effects on the energetics of the interaction (59). These factors have been evaluated recently for human immunodeficiency virus protease, a particular system for which detailed structural and thermodynamic data are available for several inhibitors that displace a highly ordered water molecule. In this case, significant contributions were found for each of these factors described above with large and partially off-setting enthalpic and entropic contributions and with the overall result that release of a bound water only marginally contributed to the overall free energy of ligand binding (59, 60).

For class II MHC proteins, detailed thermodynamic data on the energetics of peptide interaction are not available because the elaborate kinetic pathway (61–64) and presence of multiple slowly converting MHC conformations (35, 64, 65) have precluded equilibrium thermodynamic analysis. In the absence of detailed thermodynamic data, we can use existing information to help understand the role of water binding in P6/P7 region. Only one of the four water molecules bound in the P6/P7 region could be displaced productively. In addition to forming a hydrogen bond with the peptide P7 amide nitrogen, this water molecule usually forms hydrogen bonds to two other buried water molecules in the vicinity and also to MHC Glu-β28 (Fig. 7*B*). The *N*-methyl substitution displaces the water molecule, but the local hydrogen-bonding network rearranges slightly so that the only net loss is the hydrogen bond to Glu-β28 with the gain of a new hydrogen bond to the peptide backbone P7 carbonyl oxygen (Fig. 7*A*). Both Glu-β28 and the P7 carbonyl form additional hydrogen bonds, not shown in Fig. 7, with Arg-β71 and Asn-α69, respectively. Thus, the *N*-methyl substitution apparently did not result in significant loss of favorable hydrogen-bonding interactions. No significant conformational changes were observed as a result of the substitution, suggesting that both peptides are able to effect the ligand-induced conformational change in the empty MHC protein that helps to trap peptides in the binding site (35). Finally, it is not likely that nearby side chains change their ionization state as a result of the *N*-methyl introduction because the only ionizable groups in the vicinity are Glu-β28 and Arg-β74, which form a buried salt bridge that would not be affected by the substitution. Overall, it appears that for the water molecule displaced by P7 *N*-methylation, the favorable entropic contribution resulting from displacement of the bound water is sufficient to overcome other potentially offsetting contributions resulting from the substitution. For the other water molecules bound in the P6/P7 pocket, this would not appear to be the case. We attempted to displace additional water molecules by enlarging the *N*-alkyl substitution (Fig. 5). Modeling studies (data not shown) had indicated that the modifications introduced would be able to displace additional water molecules in low energy conformers without large steric clashes. However, enlarging the *N*-alkyl substitution did not result in increased binding affinity. In displacement of additional water, other effects apparently oppose an increase in binding affinity. Probable candidates for such effects would include unsatisfied hydrogen bond donors or acceptors left behind by displacement of water molecules that bridge between the MHC and bound peptide.

The P7 *N*-methyl substitution described here might be of general use in improving weakly binding peptides. Moreover, the change in backbone chemistry might also increase the resistance to proteolysis *in vivo*, which could be important in potential immunotherapy applications. Although the *N*-methyl substitution is completely buried beneath the peptide, in several cases, buried substitutions have been shown to alter T-cell activation, presumably as a result of subtle internal structural changes transmitted to the surface. For example, in the case of HLA-DR1, alterations of the completely buried P1 side chain can affect T-cell recognition (66). In the context of another class II MHC protein, I-E(k), substitution of the buried MHC residue β29 (β28 in HLA-DR1, see Fig. 7) altered T-cell recognition (67). The side chain of β29 forms one of the hydrogen bonds to the water displaced by the *N*-methyl substitution described here. The lack of such disruption of T-cell activation observed here shows that the *N*-methyl substitution is well tolerated and is consistent with the lack of detectable alteration in the crystal structure. In summary, we have shown that the binding affinity of peptides for the class II MHC protein HLA-DR1 can be increased by incorporating *N*-methyl amino acids at position 7 in the peptide without alteration of the antigenic T-cell interaction. The ability to increase the affinity of biologically relevant peptides that bind weakly to HLA-DR1 could serve as tool for the design of potential therapeutic synthetic peptides.

Acknowledgments—We thank J. Bill for the HA1.7 hybridoma and Eric R. Schreiter for data collection assistance.

REFERENCES

1. McFarland, B. J., Katz, J. F., Beeson, C., and Sant, A. J. (2001) *Proc. Natl. Acad. Sci. U. S. A.* **98,** 9231–9236
2. Watts, C. (1997) *Annu. Rev. Immunol.* **15,** 821–850
3. Rudensky, A., Preston-Hurlburt, P., Hong, S. C., Barlow, A., and Janeway, C. A., Jr. (1991) *Nature* **353,** 622–627
4. Chicz, R. M., Urban, R. G., Lane, W. S., Gorga, J. C., Stern, L. J., Vignali, D. A., and Strominger, J. L. (1992) *Nature* **358,** 764–768
5. Stern, L. J., Brown, J. H., Jardetzky, T. S., Gorga, J. C., Urban, R. G., Strominger, J. L., and Wiley, D. C. (1994) *Nature* **368,** 215–221
6. Li, Y., Li, H., Martin, R., and Mariuzza, R. A. (2000) *J. Mol. Biol.* **304,** 177–188
7. Ghosh, P., Amaya, M., Mellins, E., and Wiley, D. C. (1995) *Nature* **378,** 457–462
8. Bolin, D. R., Swain, A. L., Sarabu, R., Berthel, S. J., Gillespie, P., Huby, N. J., Makofske, R., Orzechowski, L., Perrotta, A., Toth, K., Cooper, J. P., Jiang, N., Falcioni, F., Campbell, R., Cox, D., Gaizband, D., Belunis, C. J., Vidovic, D., Ito, K., Crowther, R., Kammlott, U., Zhang, X., Palermo, R., Weber, D., Guenot, J., Nagy, Z., and Olson, G. L. (2000) *J. Med. Chem.* **43,** 2135–2148
9. Lee, K. H., Wucherpfennig, K. W., and Wiley, D. C. (2001) *Nat. Immunol.* **2,** 501–507
10. Mullen, M. M., Haan, K. M., Longnecker, R., and Jardetzky, T. S. (2002) *Mol. Cell* **9,** 375–385
11. Fremont, D. H., Dai, S., Chiang, H., Crawford, F., Marrack, P., and Kappler, J. (2002) *J. Exp. Med.* **195,** 1043–1052
12. Liu, X., Dai, S., Crawford, F., Fruge, R., Marrack, P., and Kappler, J. (2002) *Proc. Natl. Acad. Sci. U. S. A.* **99,** 8820–8825
13. Lang, H. L., Jacobsen, H., Ikemizu, S., Andersson, C., Harlos, K., Madsen, L., Hjorth, P., Sondergaard, L., Svejgaard, A., Wucherpfennig, K., Stuart, D. I., Bell, J. I., Jones, E. Y., and Fugger, L. (2002) *Nat. Immunol.* **3,** 940–943
14. Murthy, V. L., and Stern, L. J. (1997) *Structure* **5,** 1385–1396
15. Brown, J. H., Jardetzky, T. S., Gorga, J. C., Stern, L. J., Urban, R. G., Strominger, J. L., and Wiley, D. C. (1993) *Nature* **364,** 33–39
16. Hammer, J., Takacs, B., and Sinigaglia, F. (1992) *J. Exp. Med.* **176,** 1007–1013
17. Jardetzky, T. S., Brown, J. H., Gorga, J. C., Stern, L. J., Urban, R. G., Strominger, J. L., and Wiley, D. C. (1996) *Proc. Natl. Acad. Sci. U. S. A.* **93,** 734–738
18. Hennecke, J., and Wiley, D. C. (2002) *J. Exp. Med.* **195,** 571–581
19. Sundberg, E. J., Sawicki, M. W., Southwood, S., Andersen, P. S., Sette, A., and Mariuzza, R. A. (2002) *J. Mol. Biol.* **319,** 449–461
20. Krieger, J. I., Karr, R. W., Grey, H. M., Yu, W. Y., O'Sullivan, D., Batovsky, L., Zheng, Z. L., Colon, S. M., Gaeta, F. C., Sidney, J., Albertson, M., del Guercio, M., Chestnut, R. W., and Sette, A. (1991) *J. Immunol.* **146,** 2331–2340
21. De Magistris, M. T., Alexander, J., Coggeshall, M., Altman, A., Gaeta, F. C., Grey, H. M., and Sette, A. (1992) *Cell* **68,** 625–634
22. de Haan, E. C., Wauben, M. H., Grosfeld-Stulemeyer, M. C., Kruijtzer, J. A., Liskamp, R. M., and Moret, E. E. (2002) *Bioorg. Med. Chem.* **10,** 1939–1945
23. Cotton, J., Herve, M., Pouvelle, S., Maillere, B., and Menez, A. (1998) *Int. Immunol.* **10,** 159–166
24. Hill, C. M., Liu, A., Marshall, K. W., Mayer, J., Jorgensen, B., Yuan, B., Cubbon, R. M., Nichols, E. A., Wicker, L. S., and Rothbard, J. B. (1994) *J. Immunol.* **152,** 2890–2898
25. Howard, S. C., Zacheis, M. L., Bono, C. P., Welply, J. K., Hanson, G. J., Vuletich, J. L., Bedell, L. J., Summers, N. L., Schwartz, B. D., and Woulfe, S. L. (1997) *Protein Pept. Lett.* **4,** 63–68
26. Maillere, B., Mourier, G., Cotton, J., Herve, M., Leroy, S., and Menez, A. (1995) *Mol. Immunol.* **32,** 1073–1080
27. Hart, M., and Beeson, C. (2001) *J. Med. Chem.* **44,** 3700–3709
28. Stern, L. J., and Wiley, D. C. (1992) *Cell* **68,** 465–477

29. Frayser, M., Sato, A. K., Xu, L., and Stern, L. J. (1999) *Protein Expression Purif.* **15,** 105–114
30. Andersen, P. S., Lavoie, P. M., Sekaly, R. P., Churchill, H., Kranz, D. M., Schlievert, P. M., Karjalainen, K., and Mariuzza, R. A. (1999) *Immunity* **10,** 473–483
31. Nguyen, J. T., Turck, C. W., Cohen, F. E., Zuckermann, R. N., and Lim, W. A. (1998) *Science* **282,** 2088–2092
32. Figliozzi, G. M., Goldsmith, R., Ng, S. C., Banville, S. C., and Zuckermann, R. N. (1996) *Methods Enzymol.* **267,** 437–447
33. Tompkins, S. M., Rota, P. A., Moore, J. C., and Jensen, P. E. (1993) *J. Immunol. Methods* **163,** 209–216
34. Roche, P. A., and Cresswell, P. (1990) *J. Immunol.* **144,** 1849–1856
35. Zarutskie, J. A., Sato, A. K., Rushe, M. M., Chan, I. C., Lomakin, A., Benedek, G. B., and Stern, L. J. (1999) *Biochemistry* **38,** 5878–5887
36. Lamb, J. R., and Fledmann, M. (1982) *Nature* **300,** 456–458
37. Boen, E., Crownover, A. R., McIlhaney, M., Korman, A. J., and Bill, J. (2000) *J. Immunol.* **165,** 2040–2047
38. Collaborative Computational Project, N. (1994) *Acta Crystallogr. D.* **50,** 760–763
39. Otwinowski, Z., and Minor, W. (1997) *Methods Enzymol.* **276,** 307–326
40. Brunger, A. T., Adams, P. D., Clore, G. M., DeLano, W. L., Gros, P., Grosse-Kunstleve, R. W., Jiang, J.-S., Kuszewski, J., Nilges, M., Pannu, N. S., Read, R. J., Rice, L. M., Simonson, T., and Warren, G. L. (1998) *Acta Crystallogr. D. Biol. Crystallogr.* **54,** 905–921
41. Jones, T. A., Zou, J.-Y., Cowan, S. W., and Kjeldgaard, M. (1991) *Acta Crystallogr. A.* **47,** 110–119
42. McRee, D. E. (1999) *J. Struct. Biol.* **125,** 156–165
43. van Aalten, D. M. F., Bywater, R., Findlay, J. B. C., Hendlich, M., Hooft, R. W. W., and Vriend, G. (1996) *J. Computer Aided Molecular Design* **10,** 255–262
44. Laskowski, R. A., MacArthur, M. W., Moss, D. S., and Thornton, J. M. (1993) *J. Appl. Cryst.* **26,** 283–291
45. Balaban, N., and Rasooly, A. (2000) *Int. J. Food Microbiol.* **61,** 1–10
46. Redpath, S., Alam, S. M., Lin, C. M., O'Rourke, A. M., and Gascoigne, N. R. (1999) *J. Immunol.* **163,** 6–10
47. Sette, A., Alexander, J., Ruppert, J., Snoke, K., Franco, A., Ishioka, G., and Grey, H. M. (1994) *Annu. Rev. Immunol.* **12,** 413–431
48. Vargas, L. E., Parra, C. A., Salazar, L. M., Guzmán, F., Pinto, M., and Patarroyo, M. E. (2003) *BBRC*, in press
49. Brand, D. D., Whittington, K. B., and Rosloniec, E. F. (2001) *Autoimmunity* **34,** 133–145
50. Stratmann, T., Apostolopoulos, V., Mallet-Designe, V., Corper, A. L., Scott, C. A., Wilson, I. A., Kang, A. S., and Teyton, L. (2000) *J. Immunol.* **165,** 3214–3225
51. Kjellen, P., Brunsberg, U., Broddefalk, J., Hansen, B., Vestberg, M., Ivarsson, I., Engstrom, A., Svejgaard, A., Kihlberg, J., Fugger, L., and Holmdahl, R. (1998) *Eur. J. Immunol.* **28,** 755–767
52. Lam, P. Y., Jadhav, P. K., Eyermann, C. J., Hodge, C. N., Ru, Y., Bacheler, L. T., Meek, J. L., Otto, M. J., Rayner, M. M., Wong, Y. N., Chang, C.-H., Weber, P. C., Jackson, D. A., Sharpe, T. R., and Erickson-Vütanen, S. (1994) *Science* **263,** 380–384
53. Connelly, P. R., Aldape, R. A., Bruzzese, F. J., Chambers, S. P., Fitzgibbon, M. J., Fleming, M. A., Itoh, S., Livingston, D. J., Navia, M. A., Thomson, J. A., and Wilson, K. P. (1994) *Proc. Natl. Acad. Sci. U. S. A.* **91,** 1964–1968
54. Gregoriou, M., Noble, M. E., Watson, K. A., Garman, E. F., Krulle, T. M., de la Fuente, C., Fleet, G. W., Oikonomakos, N. G., and Johnson, L. N. (1998) *Protein Sci.* **7,** 915–927
55. Fan, E., Merritt, E. A., Zhang, Z., Pickens, J. C., Roach, C., Ahn, M., and Hol, W. G. (2001) *Acta Crystallogr. D. Biol. Crystallogr.* **57,** 201–212
56. Chung, E., Henriques, D., Renzoni, D., Zvelebil, M., Bradshaw, J. M., Waksman, G., Robinson, C. V., and Ladbury, J. E. (1998) *Structure* **6,** 1141–1151
57. Bhat, T. N., Bentley, G. A., Boulot, G., Greene, M. I., Tello, D., Dall'Acqua, W., Souchon, H., Schwarz, F. P., Mariuzza, R. A., and Poljak, R. J. (1994) *Proc. Natl. Acad. Sci. U. S. A.* **91,** 1089–1093
58. Dullweber, F., Stubbs, M. T., Musil, D., Sturzebecher, J., and Klebe, G. (2001) *J. Mol. Biol.* **313,** 593–614
59. Luque, I., and Freire, E. (2002) *Proteins* **49,** 181–190
60. Li, Z., and Lazaridis, T. (2003) *J. Am. Chem. Soc.* **125,** 6636–6637
61. Joshi, R. V., Zarutskie, J. A., and Stern, L. J. (2000) *Biochemistry* **39,** 3751–3762
62. Beeson, C., and McConnell, H. M. (1994) *Proc. Natl. Acad. Sci. U. S. A.* **91,** 8842–8845
63. Sadegh-Nasseri, S., and McConnell, H. M. (1989) *Nature* **337,** 274–276
64. Rabinowitz, J. D., Vrljic, M., Kasson, P. M., Liang, M. N., Busch, R., Boniface, J. J., Davis, M. M., and McConnell, H. M. (1998) *Immunity* **9,** 699–709
65. Schmitt, L., Boniface, J. J., Davis, M. M., and McConnell, H. M. (1999) *J. Mol. Biol.* **286,** 207–218
66. Wu, S., Gorski, J., Eckels, D. D., and Newton-Nash, D. K. (1996) *J. Immunol.* **156,** 3815–3820
67. Boehncke, W. H., Takeshita, T., Pendleton, C. D., Houghten, R. A., Sadegh-Nasseri, S., Racioppi, L., Berzofsky, J. A., and Germain, R. N. (1993) *J. Immunol.* **150,** 331–341
68. DeLano, W. L. (2002) *DeLano Scientific*, San Carlos, CA